Sensitive and robust second-harmonic interferometer for measuring the dispersion of the electro-optic coefficients in bulk materials

Article *in* Optics Letters · April 2011

DOI: 10.1364/OL.36.001437 · Source: PubMed

4 authors, including:

Tommaso Del Rosso
Pontifícia Universidade Católica do Rio de …
40 PUBLICATIONS **98** CITATIONS
SEE PROFILE

D. Grando
University of Pavia
50 PUBLICATIONS **295** CITATIONS
SEE PROFILE

Francesco Giammanco
Università di Pisa
125 PUBLICATIONS **724** CITATIONS
SEE PROFILE

Sensitive and robust second-harmonic interferometer for measuring the dispersion of the electro-optic coefficients in bulk materials

T. Del Rosso,[1,*] D. Grando,[2] P. Marsili,[1] and F. Giammanco[1]

[1]*Physics Department, University of Pisa, Largo Bruno Pontecorvo 3, I-56127 PISA, Italy*

[2]*Electronics Department, University of Pavia, Via Ferrata 1, I-27100 PAVIA, Italy and CNR-CNISM, Italy*

**Corresponding author: tommaso.delrosso@df.unipi.it*

Received January 28, 2011; revised March 13, 2011; accepted March 20, 2011;
posted March 21, 2011 (Doc. ID 141743); published April 13, 2011

Second-harmonic interferometry (SHI) is proposed for measuring the electro-optic (EO) coefficients of massive media. It combines the advantages of interferometric techniques with the mechanical stability of single-beam methods, simultaneously skimming the wavelength dispersion of the EO response. For demonstrating the effectiveness of the SHI technique, the EO coefficients r_{33}^T and r_{13}^T of the EO crystal lithium niobate are measured simultaneously at 1064 and 532 nm. © 2011 Optical Society of America

OCIS codes: 120.3180, 190.4400, 160.2100, 130.3730.

The harmonic interferometer is a common-path multicolor interferometer measuring the phase delay between harmonic beams of the same order and retrieving the information therein. While high-order harmonic interferometry has been used to resolve multielectron dynamics in processes of ionization or chemical reactions [1], second-harmonic interferometry [2] finds application in atmospheric metrology and diagnostic use in large plasma machines [3,4] or second-harmonic surface probing [5]. Very few times, these techniques have been considered for studying dielectrics [6], and they have never been applied to the characterization of the nonlinear properties of thick and massive samples. In this Letter, we describe a new technique for measuring the electro-optic (EO) coefficients in bulk materials based on a general, simple, and robust second-harmonic interferometry (SHI). To demonstrate the technique, we measured the EO coefficients of lithium niobate, a synthetic crystal with outstanding nonlinear and EO properties, widely employed for signal modulation and switching and sensing in commercial and prototype devices [7,8].

The EO coefficients of dielectric crystals are usually assessed through Michelson or Mach–Zehnder interferometry or via single-beam techniques such as polarimetry or ellipsometry [9]. Other demonstrated methods range, e.g., from EO beam deflection [9] to EO induced modulation of second-harmonic signals [10] and two-beam interference in photorefractive materials [11]. The accuracy of the aforementioned techniques is improved when the EO properties are probed via alternating current (AC) electric fields and phase related signals can be processed by lock-in amplifiers or even by heterodyne detection methods. Moreover, with the application of AC voltages, the influence of photorefractive space charge screening fields can be made negligible [12]. Single-beam polarimetric-ellipsometric methods often return the value of effective and not individual EO coefficients. Hence, despite the intrinsic alignment and mechanical stability problems, interferometric techniques appear to be a compulsory choice for independently measuring all components of the EO tensor. We report here, for the first time (to our knowledge), on a measuring technique that combines the advantages of the interferometric methods with the mechanical stability of single-beam procedures, simultaneously skimming the wavelength dispersion of the EO response. The proposed technique, when compared with other interferometric ones, offers comparable accuracy with the genuine advantage of a simple one-path alignment and long-time stability. In a typical SHI, the second harmonic of a laser beam is generated in a single-pass frequency converter. The fundamental beam and second-harmonic beam (SHB) propagate collinearly through a dispersive sample and, subsequently, through a second frequency converter, where the fundamental beam generates a second collinear SHB. The two SHBs interfere owing to the phase difference induced by wavelength dispersion [4]. When considering an EO dispersive sample, the EO phase shift experienced by the first SHB is given by $(4\pi/\lambda)(\Delta n_{2\omega}L + n_{2\omega}\Delta L)$, where λ and ω are the wavelength and angular frequency of the fundamental beam, $n_{2\omega}$ is the refractive index at the harmonic wavelength, L is the beam path in the sample, $\Delta n_{2\omega}$ is the EO refractive index variation at the harmonic wavelength, and ΔL is the path length variation induced by piezoelectric strain. Consistently, the EO phase shift of the fundamental beam is $(2\pi/\lambda)(\Delta n_{\omega}L + n_{\omega}\Delta L)$, and the subsequently generated second SHB carries twice the EO phase shift experienced by the fundamental beam [4,13]. The phase difference between the two SHBs can be written as $\Delta\phi + \Delta\phi_0$, where $\Delta\phi = (4\pi/\lambda)[(\Delta n_{\omega} - \Delta n_{2\omega})L + (n_{\omega} - n_{2\omega})\Delta L]$ is the EO phase shift and $\Delta\phi_0$ includes all dispersive contributions that are independent from the applied electric field.

In our SHI, sketched in Fig. 1, a linearly polarized cw Nd:YAG laser ($\lambda = 1064$ nm) with 1 W maximum power is frequency converted in two type I BIBO crystals (Red Optronics), having their optical axis parallel to one another for technical convenience. The linear polarization of the fundamental and SHB generated by the first BIBO crystal can be rotated by 90° independently by means of two dual-wavelength wave plates (DWPs; DWP(ω_A, ω_B), half-wave at ω_A and full-wave at ω_B) for probing the different elements of the EO tensors. The power of the SHB impinging on the sample is limited to a few microwatts with a beam diameter of 2 mm, whereas the fundamental

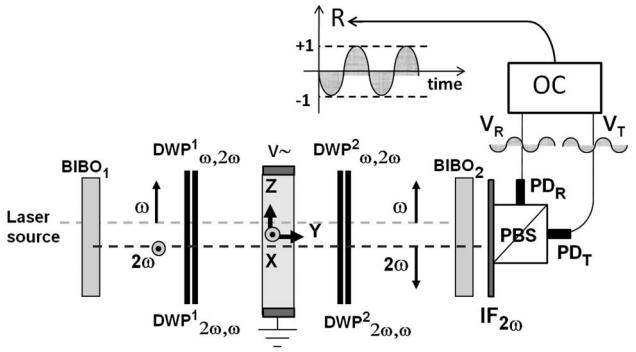

Fig. 1. The polarization state ($\uparrow, \bullet$) of the fundamental beam (ω) and the SHB (2ω) impinging on the EO crystal sample and the crystal $BIBO_2$ are individually controlled by two sets of two DWPs.

beam power is of the order of 400 mW. After the sample, a second set of two DWPs make the polarization of the fundamental beam and the SHB parallel to one another. The fundamental beam generates a second SHB in the second BIBO crystal. When the orthogonally polarized SHBs pass through a polarizing beam splitter (PBS), with its axis oriented at 45° to the SHB polarization vectors, the transmitted and reflected SHBs show a complementary interference pattern with maximized fringe visibility. The transmitted and reflected SHBs are focused on Si-PIN photodiodes equipped with low-noise variable gain amplifiers (FEMTO/LPCA-200). The intensity of each SHB can be written as $\beta_i P_0^2$, where P_0 is the fundamental beam power and β_i with $i = 1, 2$ takes into account the different SHG efficiencies of the two crystals. Assuming perfectly overlapped SHB wavefronts and defining $V_{T,R}$ as the signals detected by the two photodiodes, whose responsivity is $\alpha_{T,R}$, the information on the EO phase difference $\Delta\phi$ can be retrieved by measuring the fringe contrast, which, at the first order in α, is given by

$$R = \frac{V_T - V_R}{V_T + V_R} = C\sin(\Delta\phi + \Delta\phi_0) + \alpha, \qquad (1)$$

where $\alpha = (\alpha_T - \alpha_R)/(\alpha_T + \alpha_R)$ and the fringe visibility $C = 2(\beta_1\beta_2)^{1/2}/(\beta_1 + \beta_2)$. In this work, contrary to previous ones [4,13], the contrast R is computed using a homemade operational circuit (OC) with a bandwidth >50 kHz. The OC calculates R by combining the signal $V_{T,R}$ and amplifies it by a factor $G = 10.0 \pm 0.1$, so that it can be directly detected through a digital oscilloscope. The offset phase shift $\Delta\phi_0$ is controlled by a rotating glass slide not shown in Fig. 1. After an accurate calibration of the SHI performed as in [13], $\Delta\phi_0$ is set to the millirad level, α is adjusted to less than 1%, and the measured contrast simplifies as $R = C\sin(\Delta\phi)$. Theoretically, C should be 1; in practice, however, its maximum value is limited by the beam walk-off and crystal misalignment. Therefore, as a rule of thumb, the distance between the first converter and the PBS has to be minimized in order to maximize C and the fringe contrast. In our experiment, the maximized value of C was 0.9 with a 2% accuracy, limited by the long-time temperature fluctuations of the environment. The effectiveness of the proposed technique was demonstrated by measuring the EO coefficients of a congruent lithium niobate crystal (Crystal Growth Laboratory, UAM-Spain). The crystal was cut and polished as a rectangular prism. Silver painted electrodes were deposited on the two crystal facets perpendicular to the z axis and spaced by $d = 2.85$ mm. The beam propagation direction was parallel to the crystal y axis with the path length $L = 1.64$ mm. The maximum amplitude of the AC voltage applied to the sample was $V_M = 100$ V. The frequency of the AC voltage, 1 kHz, was well below the fundamental frequencies of the acoustic resonances of the sample; hence, the EO phase shift is related to constant stress EO coefficients, r^T [9]. Lithium niobate belongs to the trigonal system, class 3 m, and has four independent EO coefficients: $r_{13} = r_{23}$, r_{33}, $r_{51} = r_{42}$, and $r_{22} = -r_{12} = r_{61}$. When an AC voltage is applied along the crystal z axis and the beam propagation direction is along the y axis, the EO-induced phase difference measured by mean of SHI depends on the EO coefficients r_{33} and/or r_{13} at the fundamental and harmonic wavelength, and it is given by the relation

$$\Delta\phi_{ij} = \frac{4\pi}{\lambda}\left\{-\frac{1}{2}[n_{i\omega}^3 r_{i3}(\omega) - n_{j2\omega}^3 r_{j3}(2\omega)] + p\right\}\frac{V}{d}L. \qquad (2)$$

The indices i, j are equal to 1 when the beam polarization is parallel to the x axis and equal to 3 when it is parallel to the z axis; r_{ij} coincides with the constant stress EO coefficient r_{ij}^T, p equals $(n_{i\omega} - n_{j2\omega})d_{32}$, where $d_{32} = d_{31}$ is the piezoelectric coefficient, which is not affected by wavelength dispersion. In lithium niobate, $d_{32} = -0.85$ pm/V [14] and its contribution to the measured phase shift can be disregarded, as it never exceeds 0.5%. By properly arranging the polarization of the fundamental beam and the SHB traveling in the crystal, the four phase differences $\Delta\phi_{11}$, $\Delta\phi_{13}$, $\Delta\phi_{31}$, and $\Delta\phi_{33}$ can be measured, leading to four equations for the related unknown set of EO coefficients $r_{13}(\omega)$, $r_{33}(\omega)$, $r_{13}(2\omega)$, and $r_{33}(2\omega)$. Only three of the phase equations are linearly independent, as the matrix associated with the linear system of phase equations in Eq. (2) has rank 3. Hence, three EO coefficients can be determined as function of the fourth. Sometimes, the information on the relative value and wavelength dispersion of the EO coefficients is sufficient, particularly when one of them is known from the literature or can be measured independently. We measured $r_{13}(2\omega)$ independently by easily turning our SHI into a two-arm Mach–Zehnder interferometer, where the fundamental beam travels in the reference arm and the SHB solely propagates in the sample arm undergoing the EO phase shift. $r_{13}(2\omega)$ resulted to be (10.3 ± 0.3) pm/V.

Figure 2 shows the contrast signal R (bottom trace), the applied voltage V (middle trace), and the clock signal (top trace) as a function of time in the case of $\Delta\phi_{13}$. The value of the phase difference $\Delta\phi_{13}$, as derived from the data in Fig. 2, is (-62 ± 2) mrad, corresponding to a normalized phase shift for 1 V amplitude voltage of $\Delta\psi_{13} = (-0.62 \pm 0.02)$ mrad. By following analogous procedures, the other three normalized phase differences were evaluated to be $\Delta\psi_{33} = (0.18 \pm 0.005)$, $\Delta\psi_{31} = (0.87 \pm 0.03)$, and $\Delta\psi_{11} = (0.087 \pm 0.003)$ mrad. The uncertainty on the measured phases is about 3%, with major contributions from the calibration factor of the SHI and the gain G of the OC. The solution of the linear algebraic

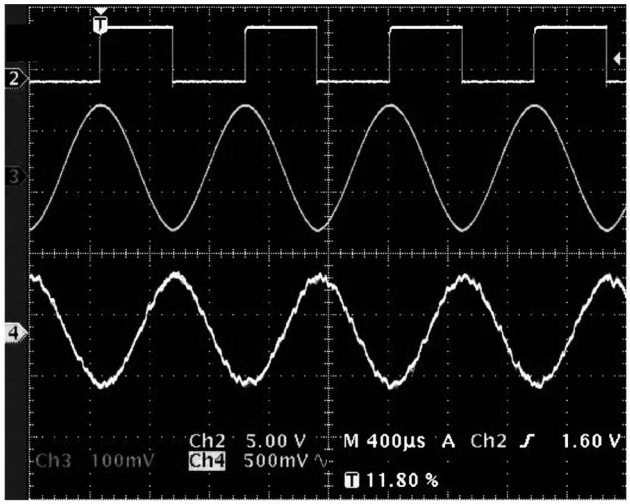

Fig. 2. Snapshot of the monitor of the oscilloscope recording the contrast R (bottom trace), the applied voltage divided by a factor 100 (middle trace), and the clock signal (top trace) in the case of $\Delta\phi_{13}$.

system involving three of the measured phase differences and related Eq. (2) leads to $r_{13}(\omega) = (9.6 \pm 0.4)\,\mathrm{pm/V}$, $r_{33}(\omega) = (30.8 \pm 0.9)\,\mathrm{pm/V}$, and $r_{33}(2\omega) = (32.6 \pm 1.0)\,\mathrm{pm/V}$, with $r_{13}(2\omega) = (10.3 \pm 0.3)\,\mathrm{pm/V}$.

In conclusion, we demonstrate a sensitive, compact, one-path, and long-time stable SHI for the simultaneous determination of the EO coefficients of transparent crystals at the fundamental and second-harmonic frequency of a near-IR cw laser beam. Although many EO crystals are photorefractive materials, the stability of the power of our laser source and the application of AC electric fields assure that the photorefractive effect has a negligible influence on the measurement of the phase-differences also when the intensity of the fundamental and SHB is higher than in our experiments [12,15]. Without using any thermal stabilization and lock-in assisted detection, the r_{13} and r_{33} EO coefficients of lithium niobate were assessed with 3% accuracy. Their values resulted to be consistent with [16] (see [16] for a comparison of $r_c = r_{33} - (n_1/n_3)^3 r_{13}$) in fair agreement with [17,18]. The sensitivity of the SHI is of the order of 1 mrad [4,13] and could be further increased by the use of a lock-in amplifier. Moreover, with the disposability of a tuneable near-IR laser source, the dispersion of the EO response could be promptly characterized in the wide wavelength range allowed by the transparency and frequency-doubling properties of BIBO crystals. The one-path configuration of the interferometer is sturdy and insensitive to mechanical vibrations. This feature makes it suitable for monitoring the time decay of the second-order optical susceptibility $\chi^{(2)}$ or developing scanning microscopes for $\chi^{(2)}$ mapping, with application in the characterization of poled polymer thin films and ferroelectric domain engineered materials.

References

1. O. Smirnova, Y. Mairesse, S. Patchkovskii, N. Dudovich, D. Villeneuve, P. Corkum, and M. Y. Ivanov, Nature **460**, 972 (2009).
2. F. Hopf, A. Tomita, and G. Al-Jumaily, Opt. Lett. **5**, 386 (1980).
3. P. D. Henshaw and D. P. DeGloria, J. Vac. Sci. Technol. B **14**, 3955 (1996).
4. F. Brandi and F. Giammanco, Opt. Lett. **32**, 2327 (2007).
5. O. Sato, R. Baba, K. Hashimoto, and A. Fujishima, J. Phys. Chem. **95**, 9636 (1991).
6. S. P. Velsko and D. Eimerl, Appl. Opt. **25**, 1344 (1986).
7. E. L. Wooten, K. M. Kissa, A. Yi-Yan, E. J. Murphy, D. A. Lafaw, P. F. Hallemeier, D. Maack, D. V. Attanasio, D. J. Fritz, G. J. McBrien, and D. E. Bossi, IEEE J. Sel. Top. Quantum Electron. **6**, 69 (2000).
8. T. Del Rosso, G. Margheri, S. Sottini, S. Trigari, M. De Sario, F. Prudenzano, and D. Grando, IEEE Sens. J. **7**, 417 (2007).
9. A. Yariv and P. Yeh, *Optical Waves in Crystals* (Wiley, 1984).
10. B. Kamg, B. K. Rhee, and G.-T. Joo, Mater. Lett. **60**, 2306 (2006).
11. M. Zgonik, K. Nakagawa, and P. Guenter, J. Opt. Soc. Am. B **12**, 1416 (1995).
12. A. Grunnet-Jepsen, I. Aubrecht, and L. Solymar, J. Opt. Soc. Am. B **12**, 921 (1995).
13. F. Brandi, F. Giammanco, W. S. Harris, T. Roche, E. Trask, and F. J. Vessel, Rev. Sci. Instrum. **80**, 113501 (2009).
14. K.-H. Kellwege and A. M. Hellwege, eds., *Landolt-Börnstein: Numerical Data and Functional Relationships in Sciences and Technology* (Springer-Verlag, 1979), Vol. 11.
15. K. Peithmann, A. Wiebrock, and K. Buse, Appl. Phys. B **68**, 777 (1999).
16. M. Abarkan, J. P. Salvestrini, M. D. Fontana, and M. Aillerie, Appl. Phys. B **76**, 765 (2003).
17. D. Grando, V. Bermudez, E. Dieguez, P. Galinetto, M. Marinone, F. Rossella, E. Giulotto, and G. Samoggia, in *Proceedings of 8° Convegno Nazionale Strumentazione e Metodi di Misura Elettroottici* (Associazione Italiana di Elettrotecnica, 2004), pp. 302–305.
18. A. Mendez, A. Garcia-Cabanes, E. Dieguez, and J. M. Cabrera, Electron. Lett. **35**, 498 (1999).